

Increased fiber communications bandwidth from a resonant cavity light emitting diode emitting at $\lambda=940$ nm

N. E. J. Hunt, E. F. Schubert, R. F. Kopf, D. L. Sivco, A. Y. Cho, and G. J. Zydzik
AT&T Bell Laboratories, Murray Hill, New Jersey 07974

(Received 3 May 1993; accepted for publication 7 September 1993)

Substrate-emitting InGaAs/AlGaAs resonant cavity light emitting diodes (RCLEDs) emitting at $\lambda=940$ nm have been fabricated for use in optical communications. The devices exhibit a high output efficiency, with a far-field intensity of $85 \mu\text{W}/\text{Steradian}$ from a planar surface at a current of 14 mA. The spontaneous spectrum exhibits a very narrow peak of only 5 nm width, as opposed to the 50-nm-wide peak of an 875 nm wavelength reference LED. We show that the narrow spectrum drastically reduces the effects of chromatic dispersion within a 3.37 km length of $62.5 \mu\text{m}$ core graded index multimode fiber. The resulting -3 dB frequency is 102 MHz for the RCLED and fiber system, as opposed to only 33 MHz for the chromatic dispersion limited reference device.

Light emitting diodes (LEDs) are widely used as sources in short and medium distance optical fiber communications¹ because of their reliability, low cost, and temperature insensitivity. There is considerable interest, therefore, in improving the efficiency and communication bandwidth in LED based fiber systems. In this work, resonant cavity light emitting diodes² (RCLEDs) have been fabricated at 940 nm with high efficiency and narrow spectral width. The narrow spectral width dramatically reduces the chromatic dispersion in glass fibers, resulting in a transmission bandwidth for the RCLED of 200 Mbit/s through 3.37 km of graded-index multimode fiber. This is 3 times the transmission bandwidth observed through the same length of fiber from a reference 875 nm LED¹ used in the commercial ODL50 optical data links. The system speed of this GaAs-based system is therefore comparable to the speed of InP-based systems operating at the $\lambda=1.3 \mu\text{m}$ glass-dispersion minimum. The light from the RCLED can be detected by silicon, germanium, or InGaAs detectors.

The design of the RCLED is given in Fig. 1. The intrinsic active region consists of four $\text{In}_{0.16}\text{Ga}_{0.84}\text{As}$ quantum wells with $\text{Al}_{0.2}\text{Ga}_{0.8}\text{As}$ barriers. The back reflecting mirror (reflectivity $R_{\text{back}} \approx 0.95$) consists of a 100-nm-thick evaporated silver layer, which also acts as a nonalloyed ohmic contact. The bottom mirror is a distributed Bragg reflector (DBR) consisting of 12 periods of alternating quarter wavelength ($\lambda/4$) layers of AlAs and GaAs. The interface between the AlAs and GaAs mirror layers is a graded composition of AlGaAs for a distance of 200 Å. The DBR is designed with a peak reflectivity of $R_{\text{out}} \approx 0.90$ at about 940 nm wavelength. The quantum wells are positioned in the antinode³ of the optical emission mode in order to increase the emission intensity by up to a factor of 2 compared to a thick active region. Light emission is through the GaAs substrate, which is antireflection coated with evaporated cubic zirconia.

By placing the active region in a Fabry-Perot cavity, the emission rate and spectrum of the emitting region is modified.⁴ In the normal direction, the emission rate at the resonance wavelength of the cavity is enhanced, while the emission rate at off-resonance wavelengths are suppressed.

By designing the resonance wavelength to coincide with the emission peak of 940 nm, we enhance the emission intensity. Two important design conditions must be met for maximum power and temperature insensitivity:

$$(1 - R_{\text{out}}) > (1 - R_{\text{back}}), \quad (1)$$

$$\xi(2\alpha L) < (1 - R_{\text{out}}). \quad (2)$$

The first design condition states that the transmission of the output mirror must be greater than the transmission of the back mirror in order to couple the majority of light into the output direction. Given that αL is the single-pass absorption of the active region at low pump with no cavity effects, the second design condition states that the fractional round-trip absorption loss of the cavity must be less than the output-mirror transmission. The factor ξ is an antinode enhancement factor which has a value of 1 for a

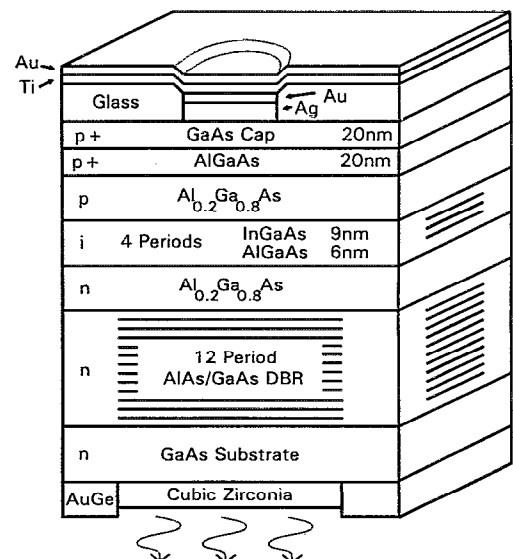


FIG. 1. The structure of a resonant cavity light emitting diode (RCLED) emitting at $\lambda=940$ nm. The 20- μm -diam Ag layer acts as a contact and back reflector, while a 12 period distributed Bragg reflector (DBR) acts as the output reflector. The active region consists of 4 $\text{In}_{0.16}\text{Ga}_{0.84}\text{As}$ quantum wells placed in the antinode of the resonant electric field mode.

thick active region, and 2 for a thin active region placed exactly in an electric field antinode of the cavity standing wave, so $1 < \zeta < 2$. The second condition ensures that at all pump levels, and at all operating temperatures, the self-absorption of the cavity does not appreciably quench the cavity resonance, and therefore the output power. This lack of self-absorption is generally not met by vertical cavity surface emitting lasers (VCSELs),⁵ which results in small spontaneous emission intensities for VCSELs pumped below threshold.⁶ The condition of Eq. (2) also ensures that only a negligible fraction of the output power is contributed to by optical gain.

The antinode intensity enhancement factor ζ is about 1.8 for our structures. The peak intensity enhancement factor G_e compared to an emitter without mirrors is⁷

$$G_e = \frac{\zeta (1 + \sqrt{R_{\text{back}}})^2 (1 - R_{\text{out}}) \tau_{\text{cav}}}{2 (1 - \sqrt{R_{\text{back}} R_{\text{out}}})^2 \tau_0} \quad (3)$$

For high reflectivity values, G_e is proportional to the cavity finesse,⁸ and has a value of $G_e = 62$ for our device. Calculations⁷ show that the carrier lifetime τ_{cav} is changed by less than 10% relative to the lifetime τ_0 without cavity. This formula assumes no light reabsorption by the active material of the cavity.

The fractional spectral width of the resonance, $\Delta\lambda_0/\lambda_0$ at the vacuum-wavelength λ_0 , on axis for high mirror reflectivities is given by⁹

$$\frac{\Delta\lambda_0}{\lambda_0} = \frac{\lambda}{2L_{\text{cav}}} \left(\frac{1 - \sqrt{R_{\text{back}} R_{\text{out}}}}{\pi^4 \sqrt{R_{\text{back}} R_{\text{out}}}} \right) \quad (4)$$

This fractional width is the inverse of the quality factor of the cavity, and for our structures we get $\Delta\lambda_0 = 4.6$ nm given a calculated effective cavity length⁹ L_{cav} of 2.7λ . The output spectrum will therefore consist of a narrow peak with enhanced spectral power density. By integrating the product of the natural emission spectrum of the active medium without cavity and an enhancement spectrum, one can determine the enhancement of integrated intensity compared to a structure with no mirrors. For a cavity width $\Delta\lambda_0$ much smaller than a Gaussian-shaped natural spectral width $\Delta\lambda_N$ for the active medium, the integrated enhancement is $G_e \text{sqr}t[\pi \ln(2)] \Delta\lambda_0/\Delta\lambda_N$. For an actual natural spectrum of width 50 nm at 16 mA current, we get a factor of 8 integrated intensity enhancement in our structure. This value is verified by the observation that the RCLED intensities are about double that of devices with no bottom DBR, which are known to have an intensity enhancement¹⁰ of just less than 4. At 16 mA current, the RCLED intensity vs angle is relatively constant up to 20 deg from normal, but drops off to half the normal-incidence value at about 40 deg, making the emission lobe narrower than a standard Lambertian source.

The spectra of a typical RCLED at various operating currents are shown in the inset of Fig. 2. The spectra at 2, 8, and 16 mA exhibit almost identical widths of 5 nm (7 meV). The consistent width indicates that there is very little absorption or gain. The power vs current curve for the RCLED at 300 K is shown as the main curve in Fig. 2.

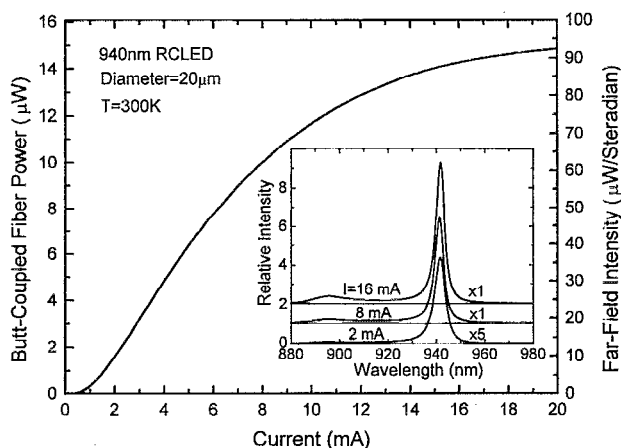


FIG. 2. The light output vs current for an RCLED at room temperature. The scale on the left shows the power butt coupled into a 62.5- μm core graded-index multimode fiber. The scale on the right shows the far-field intensity in the normal direction. The inset shows the spectra of an RCLED at three different pump currents: 2, 8, and 16 mA.

Shown is the far-field intensity in the normal direction on the right vertical axis, and the butt-coupled power into a 62.5 μm graded index multimode fiber on the left vertical axis. The output efficiency of the device is very high for currents less than 14 mA, and is in fact higher than conventional LEDs, but starts saturating at higher currents due to the effects of band filling. Given our integrated enhancement factor of 8, even further optimization of the device efficiency should be possible. Further growth optimization will also improve the > 50% reduction in power seen at 80 $^{\circ}\text{C}$ ambient temperature. The processing of an integrated lens etched into the GaAs substrate would typically increase the coupling efficiency to the fiber by a factor of 2.5–3, while only slightly increasing the coupled spectral width.

A comparison of the fiber-coupled spectra of an RCLED device and a standard 50 Mbit/s optical data link (ODL50) GaAs LED is shown in Fig. 3. The ODL50

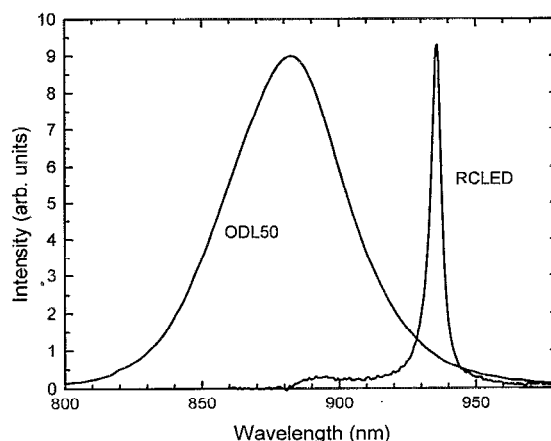


FIG. 3. A comparison of the spectral shapes of an RCLED and a reference ODL50 light emitting diode (LED) coupled into a 62.5 μm core graded-index multimode fiber. The RCLED has a spectral width of about 5 nm, while the ODL50 has a spectral width of 50 nm.

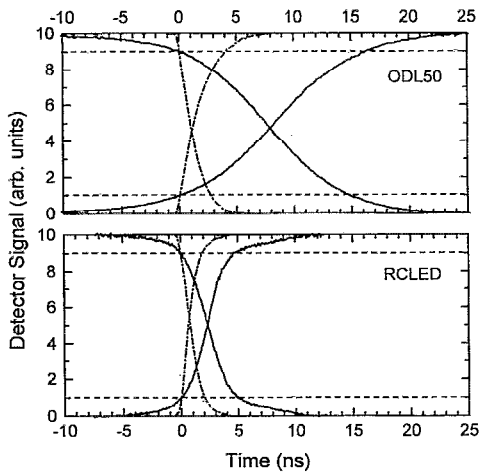


FIG. 4. Shown are the rising and falling edges of an ODL50 reference LED and an RCLED when driven by a low-frequency square wave. The dashed-dotted lines indicate the transition edges of the devices after transmission through only 5 m of fiber. The solid lines indicate the transition edges after travelling through 3.37 km of 62.5 μm core graded-index multimode fiber.

device is operating at 55 mA of current, while the RCLED is operating at 14 mA current. Both devices have a 20- μm -diam active region, are substrate emitters, have antireflection coatings, and have no coupling lens. The 6-nm-wide spectrum of the RCLED is compared to a 50-nm-wide spectrum for the ODL50 device. The narrow spectrum of the RCLED may allow it to be used in wavelength division multiplexing applications, where several signals are sent along the same fiber at slightly different wavelengths. The narrow RCLED spectrum is also important for reducing the chromatic dispersion of a signal sent over a few kilometers of optical fiber. The pulse broadening $\Delta\tau$ due to chromatic dispersion is given by

$$\Delta\tau \approx \left(\frac{1}{c} \frac{dn(\lambda_0)}{d\lambda_0} \right) l \Delta\lambda_0. \quad (5)$$

Here l is the fiber length, $\Delta\lambda_0$ is the spectral width of the source, and the bracketed term is the chromatic dispersion coefficient, which is equal to the ratio of change of the index of refraction of silica vs wavelength divided by the speed of light in vacuum. The chromatic dispersion coefficient is a fundamental property of silica fibers, and has values of about 80 ps/(km nm) at 940 nm, and about 100 ps/(km nm) at 875 nm.

The series resistance of the RCLED devices typically fall between 20 and 80 Ω , with the majority of the resistance occurring at the silver-semiconductor contact. The device bandwidth when terminated by 50 Ω resistance is measured to be 230 MHz, which agrees with the rc-limited bandwidth resulting from the parasitic capacitance of the 400- μm -wide bond pad. Devices with smaller bond pads have exhibited -3 dB frequencies of 330 MHz, and it is expected that the carrier lifetime limited speed is much greater. The rising and falling edges are shown in Fig. 4 for square wave modulation, 5 m of optical fiber, and a high speed detector. Also shown are the rising and falling edges

after transmission through 3.37 km of graded index, multimode, 62.5 μm diameter core fiber. The rise and fall times changed from about 2.0 ns with short fiber to 4.5–5 ns through the 3.37 km of fiber. The measured -3 dB frequency of the LED with 3.37 km of fiber was 102 ± 5 MHz. The bandwidth for this fiber is about 520 MHz km at this wavelength, which would result in a -3 dB frequency of 155 MHz due to mode dispersion alone. Therefore, communication rates with this RCLED are largely mode dispersion limited in commercial 62.5 μm core graded-index fiber.

In comparison to our RCLED, the rising and falling edges of a standard ODL50 GaAs light-emitting diode are also shown in Fig. 4. The rise and fall times of the LED are 2.7 and 4.0 ns, respectively. The rise and fall times for transmission through the 3.37 km of fiber, however, are 15 and 16.5 ns, respectively. Since the fiber mode dispersion is about the same as for the RCLED measurements, this large change is a result of the chromatic dispersion of the various wavelengths within the fiber. From the spectral width, one would indeed expect chromatic pulse broadening of about 17 ns for this transmission distance. The -3 dB frequency of the ODL50 LED and fiber is only 33 MHz, a factor of 3 less than for the RCLED.

In conclusion, resonant cavity light emitting diodes (RCLEDs) have been fabricated at 940 nm with high efficiency and narrow spectral width for the first time. The spectral width of 5 nm is compared to the 50 nm width of an ODL 50 reference light emitting diode LED operating at 875 nm. The narrow spectrum of the RCLED reduces the chromatic dispersion of a signal within a 3.37 km length of 62.5 μm core graded-index multimode fiber, thereby increasing the non-return-to-zero (NRZ) digital communications rate to less than 200 Mbit/s as opposed to less than 66 Mbit/s with the ODL50 reference LED.

The authors would like to acknowledge J. A. Lourenco, W. C. King, and R. H. Saul for many useful discussions.

¹R. H. Saul, T. P. Lee, and C. A. Burrus, in *Semiconductors and Semimetals* (Academic, London, 1985), Vol. 22, pp. 193–237.

²E. F. Schubert, Y.-H. Wang, A. Y. Cho, L.-W. Tu, and G. J. Zydzik, *Appl. Phys. Lett.* **60**, 921 (1992).

³T. J. Rogers, D. G. Deppe, and B. G. Streetman, *Appl. Phys. Lett.* **57**, 1858 (1990).

⁴G. Björk, S. Machida, Y. Yamamoto, and K. Igeta, *Phys. Rev. A* **44**, 669 (1991).

⁵J. L. Jewell, J. P. Harbison, A. Scherer, Y. H. Lee, and L. T. Florez, *IEEE J. Quantum Electron.* **27**, 1332 (1991).

⁶N. E. J. Hunt (unpublished).

⁷A. M. Vredenberg, N. E. J. Hunt, E. F. Schubert, D. C. Jacobson, J. M. Poate, and G. J. Zydzik, *Phys. Rev. Lett.* **71**, 517 (1993).

⁸X. P. Feng, *Opt. Commun.* **83**, 162 (1991).

⁹N. E. J. Hunt, E. F. Schubert, R. A. Logan, and G. J. Zydzik, *Appl. Phys. Lett.* **61**, 2287 (1992).

¹⁰D. G. Deppe, J. C. Campbell, R. Kuchibhotla, T. J. Rogers, and B. G. Streetman, *Electron. Lett.* **27**, 1165 (1990).